Superparamagnetic graphene oxide–Fe3O4 nanoparticles hybrid for controlled targeted drug carriers

Article *in* Journal of Materials Chemistry · April 2009

DOI: 10.1039/B821416F

6 authors, including:

Xiaoying Yang
Tianjin Medical University
60 PUBLICATIONS **3,959** CITATIONS
SEE PROFILE

Xiaoyan Zhang
Chalmers University of Technology
43 PUBLICATIONS **6,488** CITATIONS
SEE PROFILE

Yanfeng Ma
Nankai University
105 PUBLICATIONS **17,937** CITATIONS
SEE PROFILE

Yinsong Wang
Tianjin Medical University
66 PUBLICATIONS **3,091** CITATIONS
SEE PROFILE

Superparamagnetic graphene oxide–Fe_3O_4 nanoparticles hybrid for controlled targeted drug carriers

Xiaoying Yang,*[a] Xiaoyan Zhang,[b] Yanfeng Ma,[b] Yi Huang,[b] Yinsong Wang[a] and Yongsheng Chen*[b]

Received 1st December 2008, Accepted 3rd February 2009
First published as an Advance Article on the web 5th March 2009
DOI: 10.1039/b821416f

A superparamagnetic graphene oxide –Fe_3O_4 nanoparticles hybrid (GO–Fe_3O_4) was prepared *via* a simple and effective chemical precipitation method. The amount of loading of Fe_3O_4 on GO was estimated as 18.6 wt% by atomic absorption spectrometry. The hybrid was then loaded with doxorubicin hydrochloride (DXR) and the loading capacity was as high as 1.08 mg mg^{-1}. Both of the GO–Fe_3O_4 hybrids before and after loading with DXR can be dispersed well in aqueous solution. They can congregate under acidic conditions and move regularly under the force of an external magnet. Furthermore, the aggregated hybrid can be redispersed to form a stable suspension under basic conditions. These properties make it a potential candidate for controlled targeted drug delivery and release.

1 Introduction

Graphene has attracted tremendous attention because of its unique electronic,[1,2] thermal,[3] mechanical,[4] optical properties[5] and many potential applications in nanomaterials and nanotechnology. Its one-atom thickness and two-dimensional plane provide it with a large specific surface area for the immobilization of a large number of substances including a wide range of metals, biomolecules, fluorescent molecules, drugs, *etc*. For biological applications of GO, Mohanty and Berry[6] have reported the fabrication of a GO-based single-bacterium biodevice, label-free DNA sensor, bacterial DNA/protein and polyelectrolyte chemical transistor. Dai *et al* have found that the functionalized nanographene sheets are biocompatible without obvious toxicity and have employed nanographene oxide for drug delivery.[7,8] Our previous work also indicated that some anticancer drugs with aromatic systems can be loaded onto GO with high efficiency.[9] For efficient drug action, improving the drug loading efficiency is critical in drug carrier research. On the other hand, site-directed drug targeting is also very important for improving drug efficiency and decreasing the drug's side effects. Other advantages of drug targeting are the potential to reduce the amount of drugs needed (having a biological and economic impact) and the opportunity to use drugs that would otherwise not be able to be given to the patient. Graphene oxide with its two-dimensional nanostructures and adjustable surface chemistry is an excellent candidate for targeted drug delivery. One of the promising targeting methods is using magnetic particles loaded with drugs. Thus, magnetic nanoparticles have been used in various areas of biology and biomedicine including targeted drug delivery,[10–12] immunoassays,[13] hyperthermia,[14] magnetic resonance imaging contrast enhancements,[15] and the separation, purification or detection of proteins, DNA, viruses, cell, *etc*.[16–19] For biological applications, many researchers have prepared Fe_3O_4 magnetic nanoparticles with various structures or loaded them with silica,[20] polymer,[21] lipid vesicles,[22] *etc*. However, the most these Fe_3O_4 magnetic nanoparticles can achieve is only one kind of targeting transport.

Herein, we report a hybrid formed by GO with Fe_3O_4 nanoparticles by a chemical deposition method and investigate the binding of doxorubicin hydrochloride (DXR) on the hybrid. The loading amount of DXR onto GO–Fe_3O_4 can be as high as 1.08 mg mg^{-1}, although a large amount of Fe_3O_4 nanoparticles have been loaded onto GO. Furthermore, the final complex GO–Fe_3O_4–DXR possesses a hydrophilic surface and functional groups such as carboxylic groups, which may be further functionalized with other targeting molecules for realizing multi-targeted biological applications. Also, the superparamagnetic GO–Fe_3O_4 hybrid before and after loading with DXR can congregate under acidic conditions and move regularly in the magnetic field, and can be redispersed to form a stable suspension under basic conditions.

2 Experimental

Materials

Graphite was purchased from Qingdao Tianhe Graphite Co. Ltd., with an average particle diameter of 4 μm (99.95% purity). Ferric chloride hexahydrate ($FeCl_3 \cdot 6H_2O$), ferrous chloride tetrahydrate ($FeCl_2 \cdot 4H_2O$), sodium hydroxide were purchased from Tianjin No. 3 Chemical Plant. Doxorubicin hydrochloride (DXR) was purchased from Beijing Huafeng United Technology Co. Ltd. A dialysis chamber was purchased from Beijing Dingguo Biotechnology Co. (diameter = 36 mm), which had a molecular weight cutoff of 8000–15000 g mol^{-1}.

[a]*School of Pharmaceutical Sciences, Tianjin Medical University, Tianjin, 300070, China. E-mail: yangxiaoying@tijmu.edu.cn; Fax: +86 (22) 2349-9992; Tel: +86 (22) 2350-0693*
[b]*Center for Nanoscale Science and Technology and Key Laboratory of Functional Polymer Materials, Institute of Polymer Chemistry, College of Chemistry, Nankai University, Tianjin, 300071, China. E-mail: xiaoyanzhang220@mail.nankai.edu.cn; yihuang@nankai.edu.cn; maggie@nankai.edu.cn; yschen99@nankai.edu.cn; Fax: +86 (22) 2349-9992; Tel: +86 (22) 2350-0693*

Preparation of water-soluble, individual graphene oxide

Graphene oxide (GO) was prepared from purified natural graphite according to a modified Hummers method.[23] In detail, graphite powder (1 g), $NaNO_3$ (0.75 g) and $KMnO_4$ (3 g) in concentrated H_2SO_4 (75 ml) were vigorously stirred at room temperature for 7 days. On completion of the reaction, 5% H_2SO_4 (200 mL) aqueous solution was added, and the temperature was kept at 98 °C for 2 h. Then the temperature was reduced to 60 °C, H_2O_2 (30%, 6 ml) was added and the reaction was further stirred for 2 h. The above mixture was centrifuged to collect the bottom product and sequentially washed with 5% H_2SO_4/0.5% H_2O_2 (15 times), 5% HCl solution (5 times), and then washed repeatedly with distilled water until the pH of the supernatant was neutral. Finally the material was dried to obtain a loose brown powder.

Determination of the content of carboxylic acid groups of GO

The content of carboxylic acid groups of GO was determined by acid–base titration. GO (49.8 mg) was first sonicated in NaOH aqueous solution (10 mL 0.103 N) under argon for 40 min, then the solution was stirred for 48 h. The mixture was then placed into the dialysis chambers. Dialysing was continued until the dialysate became neutral. The combined dialysate was condensed using a rotary evaporator and titrated with HCl aqueous solution (6.30 mL 0.108 N) to reach the neutral point (pH 7.00), as monitored by a pH meter (pHS-3C). This gave the amount of carboxylic acid groups as 0.346 mmol for this GO sample. The amount of carbon in GO is estimated to be 4.15 mmol by assuming that GO is solely composed of carbon. The same procedure was repeated three times and the average mole percentage of the carboxylic acid groups on GO is about 8.1%.

Preparation of GO–Fe_3O_4 hybrid *via* chemical deposition

GO (40 mg) was first sonicated in 100 mL dilute NaOH aqueous solution (pH 12) for several hours to transform the carboxylic acid groups to carboxylate anions, followed by thorough dialysis until the dialysate became neutral. The resulting product was condensed to 20 mL and placed in a 50 mL round-bottom flask. The flask was then purged with N_2 for 30 min. A solution of $FeCl_3 \cdot 6H_2O$ (48.0 mg) and $FeCl_2 \cdot 4H_2O$ (763.4 mg) in water (5 mL) was purged with N_2 for 30 min and then added to the flask. The mixture was stirred overnight under N_2 for ion exchange. After a thorough washing with water consisting of several centrifugation and ultrafiltration cycles under a N_2 atmosphere to remove excess iron salts, the solid product was redispersed in 25 mL water in a two-necked round bottom flask under a N_2 atmosphere. A NaOH aqueous solution (4 mL, 3 M) was added dropwise under N_2. The mixture was kept stirring at 65 °C for a further 2 h. Then the mixture was washed thoroughly with water to neutral pH and dried under vacuum at room temperature.

Conjugation of DXR and GO–Fe_3O_4 hybrid

GO–Fe_3O_4 hybrid with the final concentration of 0.145 mg mL^{-1} was first sonicated with the desired concentration of DXR solution for 0.5 h and then stirred overnight at room temperature in the dark. All samples were ultracentrifuged at 14000 rpm for 1 h. The DXR concentration in the upper layer was measured using a standard DXR concentration curve generated with an Ultraviolet-visible-near IR spectrophotometer (UV-vis-NIR) (JASCO, V-570) at the wavelength of 233 nm from a series of DXR solutions with different concentrations. As comparison, GO was loaded with DXR under similar conditions.

Characterization

Transmission electron microscopy (TEM, FEI, TECNAI-20), atomic force microscope (AFM, Veeco, Nanoscope IV, Digital Instruments) were used to characterize the size and morphology of the samples. Fourier transform infrared spectroscopy (FT-IR) spectra were obtained using a Bruker Tensor 27 spectrometer. The magnetization curve of the GO–Fe_3O_4 hybrid was measured as a function of the applied magnetic field H with a 9600 VSM (LDJ Co.) superconducting quantum interference device (SQUID) magnetometer. The hysteresis of the magnetization was obtained by varying H between +6000 and −6000 Oe at 300 K. The composition of the GO–Fe_3O_4 hybrid was determined with atomic absorption spectrophotometer analysis (HITACHI, 180-80) and thermal gravimetric analysis (TGA) using a Netzsch STA 409PC with a heating rate of 10 °C min^{-1} from room temperature to 1000 °C under N_2. The amount of DXR loaded on to the GO–Fe_3O_4 hybrid and neat GO were determined by the method described in our previous work.[9]

3 Results and discussion

The superparamagnetic GO–Fe_3O_4 hybrid was prepared by chemical deposition of iron ions using soluble GO as carriers (Scheme 1). The method is that Fe^{3+}/Fe^{2+} ions in the proper ratio were captured by carboxylate anions on the graphene sheet by

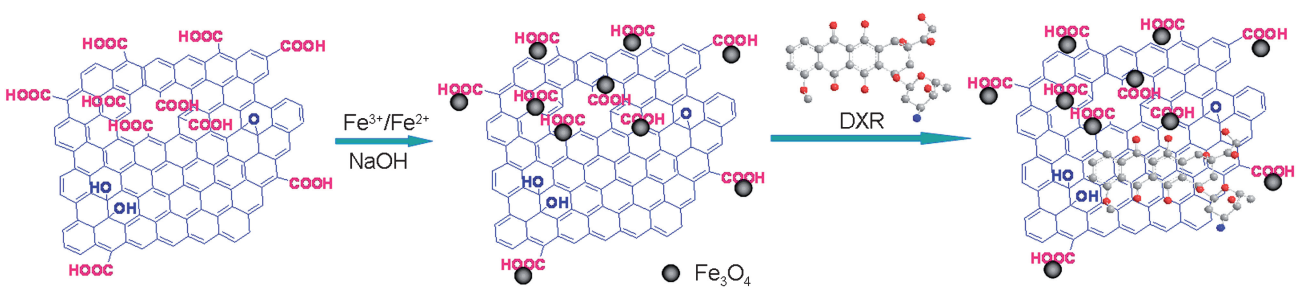

Scheme 1 Schematic representation of GO loaded with Fe_3O_4 nanoparticles and DXR

coordination and then Fe_3O_4 nanoparticles on GO were precipitated by treating iron ions coordinated with GO with aqueous NaOH solution. Generally the ratio of Fe^{3+}/Fe^{2+} ions for preparation of Fe_3O_4 nanoparticles is controlled as 2/1. Thus the content of the carboxylic acid groups on GO needs to be determined by acid–base titration method first. The average mole percentage of the carboxylic acid groups on GO we prepared is estimated at about 8.1%. As Fe^{3+} has a much higher affinity than Fe^{2+} for carboxylic groups,[24] we adopted the 2/3 mole ratio of Fe^{3+}/–COO^- with a large excess of Fe^{2+}.

As expected, Fe_3O_4 nanoparticles are chemically deposited on GO with the aid of the –COOH on GO. The large specific surface area of GO has a particular advantage of loading magnetic nanoparticles. The morphology of the GO–Fe_3O_4 hybrid was characterized with TEM and AFM. As can be seen from the TEM images (Fig. 1a), the size of the Fe_3O_4 nanoparticles on GO is 2–4 nm with a narrow size distribution, and some Fe_3O_4 aggregation is observed. From the image of AFM (Fig. 1b), GO used as the carriers of Fe_3O_4 nanoparticles show a height of ~1.0 nm, suggesting a single layer graphene sheet.[12] Many round surface protuberances with 2–4 nm height are observed on the surface of the GO–Fe_3O_4 hybrid and some aggregated Fe_3O_4 nanoparticles are also observed. Obviously, a large amount of Fe_3O_4 nanoparticles are immobilized onto the GO sheets.

The FTIR spectra of GO and GO–Fe_3O_4 hybrid are shown in Fig. 2. The peak at 1734 cm^{-1} corresponding to ν(C=O) of –COOH on the GO shifts to 1594 cm^{-1} due to the formation of –COO^- after coating with Fe_3O_4. The characteristic peak corresponding to the stretching vibration of Fe–O bond is also shifted to higher wavenumbers of 701 cm^{-1} compared to that of 570 cm^{-1} reported for the stretching mode of Fe–O in bulk Fe_3O_4,[25,26] suggesting that Fe_3O_4 is bound to the –COO^- on the GO surface.

The magnetization curve of GO–Fe_3O_4 hybrid was measured at room temperature, as shown in Fig. 3. The magnetic hysteresis loops are S-like curves. The magnetic remanence of the sample was 0.144 emu g^{-1}, nearly zero. This indicated that there was almost no remaining magnetization when the external magnetic field was removed, suggesting that GO–Fe_3O_4 exhibit a superparamagnetic behavior. The specific saturation magnetization, M_s of the sample, is 4.62 emu g^{-1}. This value is smaller than the reported value of bulk Fe_3O_4 of 92 emu g^{-1}.[27] The reduction in the value of M_s could be attributed to the rather smaller size of the Fe_3O_4 nanoparticles and the relatively low amount of Fe_3O_4 loaded on GO, which is estimated as 18.6 wt% calculated from the content of Fe by atomic absorption spectrum. However

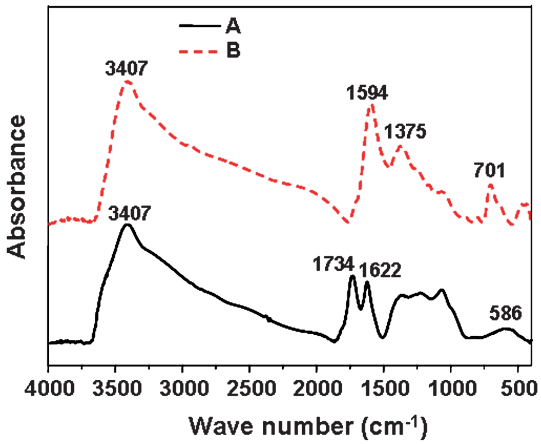

Fig. 2 FTIR spectra of GO (A) and GO–Fe_3O_4 hybrid (B).

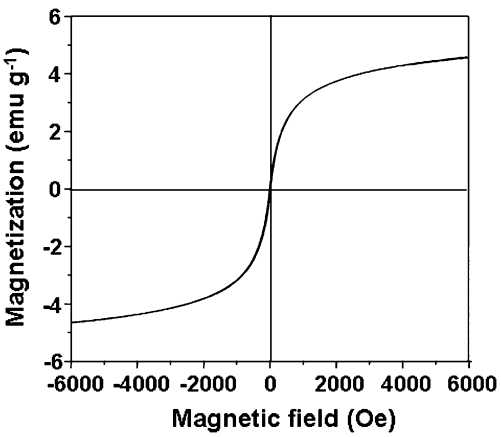

Fig. 3 Magnetization curve of GO–Fe_3O_4 hybrid.

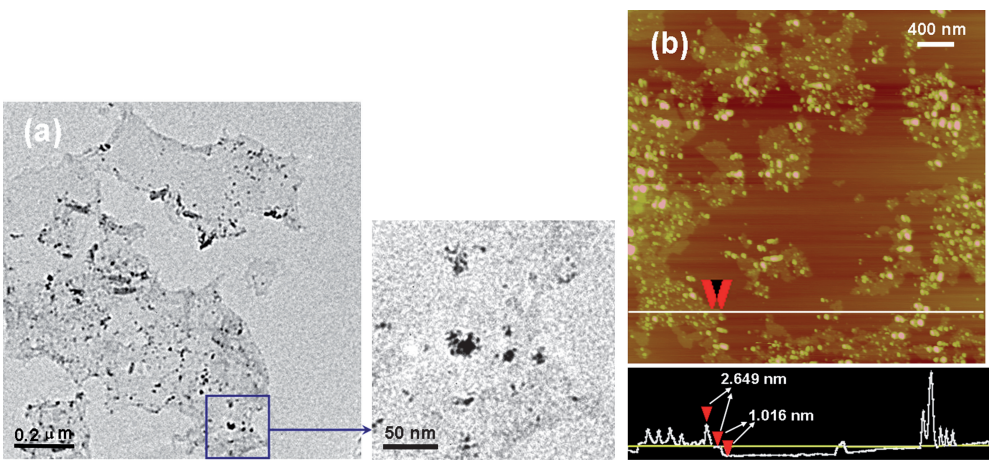

Fig. 1 TEM (a) and AFM (b) images of GO–Fe_3O_4 hybrid.

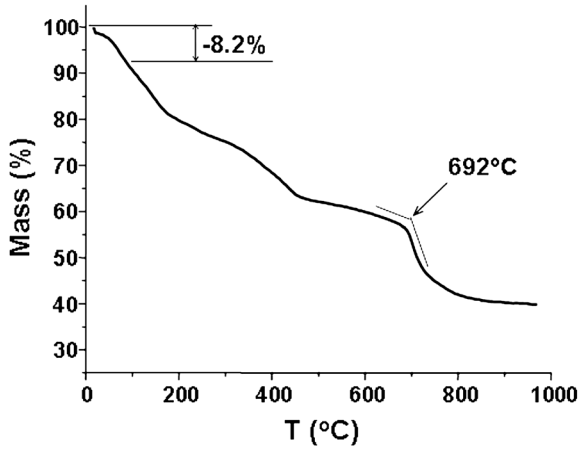

Fig. 4 Thermal gravimetric analysis of GO–Fe_3O_4.

GO–Fe_3O_4 could move regularly under the action of an external magnet after they congregated, as shown in Fig. 3.

The composition of GO–Fe_3O_4 was further characterized with TGA in a nitrogen environment, as shown in Fig. 4. For GO–Fe_3O_4, a slow weight loss (8.2 wt%) at low temperature (<100 °C) can be observed, which can be assigned to the loss of the residual or absorbed solvent. Then two stages of weight loss occurred around 150 °C and 426 °C (from a derivative thermogravimetric curve), indicating the decomposition and vaporization of various functional groups at different positions on GO. The large weight loss at the onset of 692 °C may be attributed to the breakdown of the $–COO^-$ group coordinated with Fe_3O_4 nanoparticles in the GO–Fe_3O_4 hybrid. A similar result has been observed in the preparation of polymer/Fe_3O_4 magnetic microspheres.[28] When the temperature reached 850 °C, the weight of the hybrid remained at 41.1 wt% and almost no weight loss occurred after this temperature.

The loading capacity of DXR on GO–Fe_3O_4 hybrid was determined by UV spectrum at 233 nm, which was calculated by the difference of DXR concentrations between the original DXR solution and the supernatant solution after loading. The loading amount of DXR on GO–Fe_3O_4 was investigated in different initial DXR concentrations with respect to the same concentration of GO–Fe_3O_4 (0.145 mg mL^{-1}), and the loading of DXR on neat GO is used as a comparison, as shown in Fig. 5. The saturated loading amount of DXR on GO–Fe_3O_4 is 1.08 mg mg^{-1} while the amount of DXR loaded on GO can reach 2.35 mg mg^{-1} at the DXR concentration of 0.47 mg mL^{-1}. π–π Stacking and the hydrogen bonding interaction between GO and DXR both play important roles in the high loading of DXR on GO, which has been discussed in our previous work.[9] Therefore, some surface areas on GO have obviously been occupied by Fe_3O_4 nanoparticles. However, even such a value of loading is higher than that of the other common drug carrier materials, such as polymer micelles (60 wt%),[29] hydrogel microparticles (50 wt%),[30] liposomes (8.9 wt%),[31] carbon nanohorns (20 wt%),[32] where the loading capacity is always below 1 mg mg^{-1}.

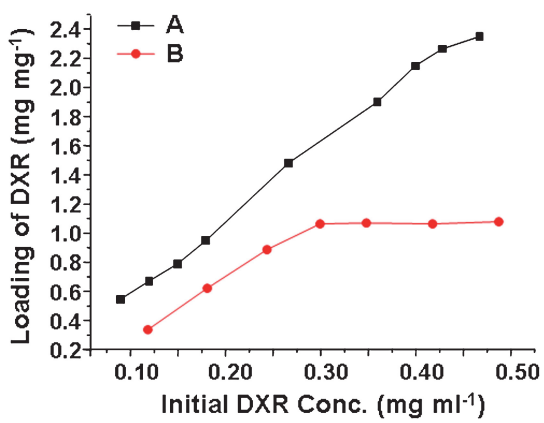

Fig. 5 Loading capacity of DXR on GO (A) and GO–Fe_3O_4 hybrid (B) in different initial DXR concentrations.

After oxidation, the graphene can be introduced with hydrophilic groups such as hydroxyl and carboxylic and it can be well-dispersed in aqueous solution.[23] As expected, the sedimentation of Fe_3O_4 magnetic nanoparticles was reduced after they were deposited onto GO. Fig. 6 shows the images of the behaviors of GO–Fe_3O_4 hybrid (upper) and GO–Fe_3O_4 hybrid loaded with DXR (lower) in the magnetic field under neutral conditions (A), acidic conditions (pH 2–3) (B–E) and basic conditions (pH 8–9) (F). GO–Fe_3O_4 hybrid (A) was the supernatant after centrifuging at 12000 rpm for 30 min. The superparamagnetic GO–Fe_3O_4 hybrid didn't move in the magnetic field under neutral conditions, suggesting good dispersion of the hybrid in water. However, it congregated immediately after adding 1–2 drops HCl (1 M) (pH 2–3) and can be moved regularly under the force of the external magnetic field. This indicates that the carboxylic acid groups are free for efficient hydrogen-bonding interaction with each other under acidic conditions. This may make it a potential pH-triggered targeting transporter for targeted therapy. When the hybrid was loaded with DXR, it showed a similar phenomenon; only the rate of congregation became slower. This may be because the epoxide and the hydroxyl groups on GO were deoxygenated during Fe_3O_4 nanoparticles deposition by treating with aqueous NaOH solution[33] and a small part of the polar groups interacted

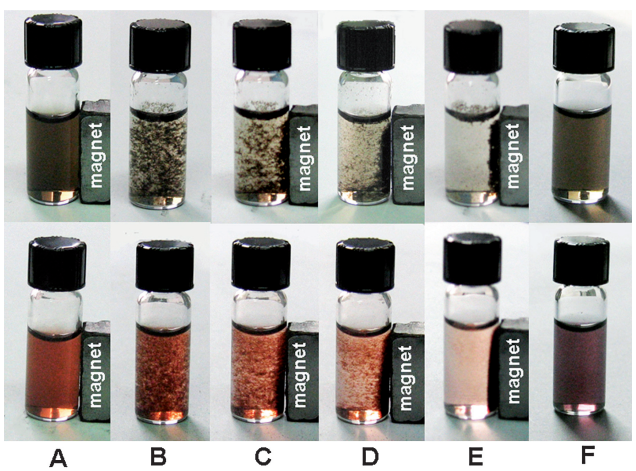

Fig. 6 Photographic images of the behaviors of GO–Fe_3O_4 hybrid (upper)[a] and GO–Fe_3O_4 hybrid loaded with DXR (lower)[b] in the magnetic field under different conditions: neutral conditions (A), acidic conditions (pH 2–3) (B–E) and basic conditions (pH 8–9) (F). (a) GO–Fe_3O_4 hybrid was the supernatant after centrifuging at 12000 rpm for 30 min; (b) GO–Fe_3O_4 hybrid loaded with DXR was suspended in water.

with –OH groups in DXR through hydrogen bonding. More remarkably, both the congregated GO–Fe_3O_4 hybrid before and after loading with DXR under acidic conditions can be redispersed and form a stable suspension after adding 2–3 drops of NaOH (1 M) (pH 8–9). This stablility can be attributed to a strengthened electrostatic stabilization under alkaline conditions, as the repulsion between negatively charged GO should increase at higher pH values. Thus, the GO–Fe_3O_4 hybrid and GO–Fe_3O_4–DXR complex can congregate and be redispersed reversibly under different pH conditions. This indicates that some functional groups on GO such as carboxylic acid groups are still free even after loading with a large amount of Fe_3O_4 nanoparticles and DXR. These free functional groups can then be used in future to other functional biomolecules or even other drugs such as antigen–antibody, folic acid, *etc*. for specific multi-targeting or multi-drug loading and delivery. This certainly indicates the huge potential applications in clinical diagnosis, separation and detection of biomolecules and as medicine transporters.

4 Conclusions

In summary, we have developed a simple, effective and scalable method to chemically deposit Fe_3O_4 nanoparticles onto GO. This hybrid can be loaded with anti-cancer drug DXR with a high loading capacity up to 1.08 mg mg^{-1}. This GO–Fe_3O_4 hybrid shows superparamagnetic property and can congregate under acidic conditions and be redispersed reversibly under basic conditions. Both the GO–Fe_3O_4 hybrid before and after loading with the molecule DXR can be moved regularly after congregating at acidic pH values by the force of an external magnetic field. This pH-triggered controlled magnetic behavior makes this material a promising candidate for controlled targeted drug delivery. Thus, these graphene-based magnetic nanoparticles, with good solubility and further functionalization capability, are expected to find practical applications in biomedicine, biomaterials separation and biodiagnostics.

Acknowledgements

We gratefully acknowledge the financial support from the NSFC (#20774047), MoST (#2006CB932702), MoE (#708020) and NSF of Tianjin City (#07JCYBJC01700, #07JCYBJC03000, #08JCZDJC25300).

References

1 K. S. Novoselov, Z. Jiang, Y. Zhang, S. V. Morozov, H. L. Stormer, U. Zeitler, J. C. Maan, G. S. Boebinger, P. Kim and A. K. Geim, *Science*, 2007, **315**, 1379.
2 Y. B. Zhang, Y. W. Tan, H. L. Stormer and P. Kim, *Nature*, 2005, **438**, 201.
3 A. A. Balandin, S. Ghosh, W. Z. Bao, I. Calizo, D. Teweldebrhan, F. Miao and C. N. Lau, *Nano Lett.*, 2008, **8**, 902.
4 C. Lee, X. D. Wei, J. W. Kysar and J. Hone, *Science*, 2008, **321**, 385.
5 K. F. Mak, M. Y. Sfeir, Y. Wu, C. H. Lui, J. A. Misewich and T. F. Heinz, *Phys. Rev. Lett.*, 2008, **101**, 196405.
6 N. Mohanty and V. Berry, *Nano Lett.*, 2008, **8**, 4469.
7 Z. Liu, J. T. Robinson, X. Sun and H. Dai, *J. Am. Chem. Soc.*, 2008, **130**, 10876.
8 X. Sun, Z. Liu, K. Welsher, J. T. Robinson, A. Goodwin, S. Zaric and H. Dai, *Nano Res.*, 2008, **1**, 203.
9 X. Yang, X. Zhang, Z. Liu, Y. Ma, Y. Huang and Y. Chen, *J. Phys. Chem. C*, 2008, **112**, 17554.
10 S. W. Cao, Y. J. Zhu, M. Y. Ma, L. Li and L. Zhang, *J. Phys. Chem. C*, 2008, **112**, 1851.
11 S. Muniyandy, B. Kesavan, M. Gomathinayagam and P. K. Sadasivan, *Int. J. Pharm.*, 2004, **283**, 71.
12 A. S. Lubbe, C. Bergemann, W. Huhnt, T. Fricke, H. Riess, J. W. Brock and D. Huhn, *Cancer Res.*, 1996, **56**, 4694.
13 J. Richardson, P. Hawkins and R. Luxton, *Biosens. Bioelectron.*, 2001, **16**, 989.
14 W. Schutt, C. Gruttner, U. Hafeli, M. Zborowski, J. Teller, H. Putzar and C. Schumichen, *Hybridoma*, 1997, **16**, 109.
15 Y. M. Huh, Y. W. Jun, H. T. Song, S. Kim, J. S. Choi, J. H. Lee, S. Yoon, K. S. Kim, J. S. Shin, J. S. Suh and J. Cheon, *J. Am. Chem. Soc.*, 2005, **127**, 12387.
16 Y. Haik, V. Pai and C. J. Chen, *J. Magn. Magn. Mater.*, 1999, **194**, 254.
17 J. Bao, W. Chen, T. Liu, Y. Zhu, P. Jin, L. Wang, J. Liu, Y. Wei and Y. Li, *Acs Nano*, 2007, **1**, 293.
18 J.-M. Nam, C. S. Thaxton and C. A. Mirkin, *Science*, 2003, **301**, 1884.
19 H. Y. Park, M. J. Schadt, L. Wang, I. S. Lim, P. N. Njoki, S. H. Kim, M. Y. Jang, J. Luo and C. J. Zhong, *Langmuir*, 2007, **23**, 9050.
20 Y. P. He, S. Q. Wang, C. R. Li, Y. M. Miao, Z. Y. Wu and B. S. Zou, *J. Phys. D: Appl. Phys.*, 2005, **38**, 1342.
21 J. Xie, C. Xu, Z. Xu, Y. Hou, K. L. Young, S. X. Wang, N. Pourmand and S. Sun, *Chem. Mater.*, 2006, **18**, 5401.
22 A. Wijaya and K. Hamad-Schifferli, *Langmuir*, 2007, **23**, 9546.
23 H. A. Becerril, J. Mao, Z. Liu, R. M. Stoltenberg, Z. Bao and Y. Chen, *Acs Nano*, 2008, **2**, 463.
24 M. Zhang, B. Wang, Y. Zhang and B. He, *Ion Exch. Adsorpt.*, 1995, **11**, 302.
25 S. F. Chin, K. S. Iyer and C. L. Raston, *Lab Chip*, 2008, **8**, 439.
26 C. Rocchiccioli-Deltche, R. Franck, V. Cabuil and R. Massart, *J. Chem. Res.*, 1987, **5**, 126.
27 J. Popplewell, L. Sakhnini and J. Magn, *Magn. Mater.*, 1995, **142**, 72.
28 J. Huang, S. Wan, M. Guo and H. Yan, *J. Mater. Chem.*, 2006, **16**, 4535.
29 Y. Chan, T. Wong, F. Byrne, M. Kavallaris and V. Bulmus, *Biomacromolecules*, 2008, **9**, 1826.
30 F. Cavalieri, E. Chiessi, R. Villa, L. Vigano, N. Zaffaroni, M. F. Telling and G. Paradossi, *Biomacromolecules*, 2008, **9**, 1967.
31 W. T. Sun, N. Zhang, A. G. Li, W. W. Zou and W. F. Xu, *Int. J. Pharm.*, 2008, **353**, 243.
32 T. Murakami, K. Ajima, J. Miyawaki, M. Yudasaka, S. Iijima and K. Shiba, *Mol Pharm.*, 2004, **1**, 399.
33 X. Fan, W. Peng, Y. Li, X. Li, S. Wang, G. Zhang and F. Zhang, *Adv. Mater.*, 2008, **20**, 1.

